

Steps in the exact time-dependent potential energy surface

Ali Abedi,¹ Federica Agostini,¹ Yasumitsu Suzuki,¹ and E.K.U. Gross¹

¹Max-Planck Institut für Mikrostrukturphysik, Weinberg 2, D-06120 Halle, Germany

(Dated: October 29, 2018)

We study the exact Time-Dependent Potential Energy Surface (TD PES) in the presence of strong non-adiabatic coupling between the electronic and nuclear motion. The concept of the TD PES emerges from the exact factorization of the full electron-nuclear wave-function [A. Abedi, N. T. Maitra, and E. K. U. Gross, Phys. Rev. Lett. **105**, 123002 (2010)]. Employing a 1D model-system, we show that the TD PES exhibits a dynamical step that bridges between piecewise adiabatic shapes. We analytically investigate the position of the steps and the nature of the switching between the adiabatic pieces of the TD PES.

PACS numbers: 31.50.-x, 82.20.Gk

The description of coupled electron-nuclear motion is one of the biggest challenges in condensed-matter physics and theoretical chemistry. Fundamental to our understanding is the adiabatic separation of electronic and nuclear motion embodied in the Born-Oppenheimer (BO) approximation. It allows one to visualize -approximately- a molecule as a set of nuclei moving on a single Potential Energy Surface (PES) generated by the electrons in a specific electronic eigenstate. The BO approximation breaks down when two or more BO PESs come close or cross. Some of the most fascinating and most challenging molecular processes occur in the regime where the BO approximation is not valid, e.g. ultrafast nuclear motion through conical intersections [1], radiationless relaxation of excited electronic states [2], intra- and inter-molecular electron and proton transfer [3], to name a few. The standard way of studying and interpreting these, so-called, "non-adiabatic" processes is to expand the full molecular wave function in terms of the BO electronic states. Within this expansion, non-adiabatic processes can be viewed as a nuclear wave packet with contributions on several BO PESs, coupled through the non-adiabatic coupling (NAC) terms which in turn induce transitions between the BO PESs. While this provides a formally exact description one may nevertheless ask: Is it also possible to study the molecular process using a *single* PES? This question is particularly relevant if one thinks of a classical or semi-classical treatment of the nuclei where a well-defined single classical force would be highly desirable.

In a recent Letter, we have introduced an exact time-dependent potential energy surface (TD PES) that, together with an exact time-dependent vector potential govern the nuclear motion. These concepts emerge from a novel way to approach the coupled electron-nuclear dynamics via an exact factorization of the electron-nuclear wave function [4]. Features of the exact TD PES were studied in the presence of strong laser fields [4, 5]. In the present Letter we investigate the generic features of the exact TD PES *without* external laser but in the presence of strong non-adiabatic couplings. A major result

will be that the exact TD PES exhibits nearly discontinuous steps connecting different static BO PESs, reminiscent of Tully's surface hopping [6] in the classical limit.

In [4] we have proved that the *exact* solution of the time-dependent Schrödinger equation (TDSE),

$$\hat{H}\Psi(\underline{\mathbf{r}}, \underline{\mathbf{R}}, t) = i\partial_t\Psi(\underline{\mathbf{r}}, \underline{\mathbf{R}}, t), \quad (1)$$

of the complete system of interacting electrons and nuclei can be written as a single product (unlike the BO expansion), $\Psi(\underline{\mathbf{r}}, \underline{\mathbf{R}}, t) = \Phi_{\underline{\mathbf{R}}}(\underline{\mathbf{r}}, t)\chi(\underline{\mathbf{R}}, t)$, of the nuclear wave-function, $\chi(\underline{\mathbf{R}}, t)$, and the electronic conditional wave-function, $\Phi_{\underline{\mathbf{R}}}(\underline{\mathbf{r}}, t)$, that satisfies the partial normalization condition (PNC), $\int d\underline{\mathbf{r}}|\Phi_{\underline{\mathbf{R}}}(\underline{\mathbf{r}}, t)|^2 = 1$. In the absence of time-dependent external fields, the system is described by the Hamiltonian \hat{H} ,

$$\hat{H} = \hat{H}_{BO}(\underline{\mathbf{r}}, \underline{\mathbf{R}}) + \hat{T}_n(\underline{\mathbf{R}}), \quad (2)$$

that contains the traditional BO electronic Hamiltonian, $\hat{H}_{BO}(\underline{\mathbf{r}}, \underline{\mathbf{R}}) = \hat{T}_e(\underline{\mathbf{r}}) + \hat{W}_{ee}(\underline{\mathbf{r}}) + \hat{V}_{en}(\underline{\mathbf{r}}, \underline{\mathbf{R}}) + \hat{W}_{nn}(\underline{\mathbf{R}})$, and the nuclear kinetic energy, $\hat{T}_n(\underline{\mathbf{R}})$. Throughout this paper we use atomic units (unless stated otherwise) and the electronic and nuclear coordinates are collectively denoted by $\underline{\mathbf{r}}$ and $\underline{\mathbf{R}}$, respectively.

The exact electronic wave-function satisfies the equation

$$\left(\hat{H}_{BO}(\underline{\mathbf{r}}, \underline{\mathbf{R}}) + \hat{U}_{en}^{coup} - \epsilon(\underline{\mathbf{R}}, t)\right)\Phi_{\underline{\mathbf{R}}}(\underline{\mathbf{r}}, t) = i\partial_t\Phi_{\underline{\mathbf{R}}}(\underline{\mathbf{r}}, t), \quad (3)$$

where the electron-nuclear coupling operator is $\hat{U}_{en}^{coup} = \sum_{\nu=1}^{N_n} ((-i\nabla_{\nu} - \mathbf{A}_{\nu}(\underline{\mathbf{R}}, t))^2/2 + (-i\nabla_{\nu}\chi/\chi + \mathbf{A}_{\nu}(\underline{\mathbf{R}}, t))(-i\nabla_{\nu} - \mathbf{A}_{\nu}(\underline{\mathbf{R}}, t)))/M_{\nu}$. The time-evolution of the nuclear wave-function is governed by the Schrödinger equation:

$$\left(\sum_{\nu=1}^{N_n} \frac{(-i\nabla_{\nu} + \mathbf{A}_{\nu}(\underline{\mathbf{R}}, t))^2}{2M_{\nu}} + \epsilon(\underline{\mathbf{R}}, t)\right)\chi(\underline{\mathbf{R}}, t) = i\partial_t\chi(\underline{\mathbf{R}}, t). \quad (4)$$

These equations lead to rigorous definitions of the TD-PES and the time-dependent vector potential

$$\epsilon(\underline{\mathbf{R}}, t) = \epsilon_{gi}(\underline{\mathbf{R}}, t) + \epsilon_{gd}(\underline{\mathbf{R}}, t) \quad (5)$$

$$\mathbf{A}_\nu(\underline{\mathbf{R}}, t) = \left\langle \Phi_{\underline{\mathbf{R}}}(t) \left| -i\nabla_\nu \Phi_{\underline{\mathbf{R}}}(t) \right\rangle_{\underline{\mathbf{r}}} \quad (6)$$

The TDPEs consists of two parts: $\epsilon_{gi}(\underline{\mathbf{R}}, t)$, defined as

$$\epsilon_{gi}(\underline{\mathbf{R}}, t) = \left\langle \Phi_{\underline{\mathbf{R}}}(t) \left| \hat{H}_{BO}(\underline{\mathbf{r}}, \underline{\mathbf{R}}) + \hat{U}_{en}^{coup}(\underline{\mathbf{r}}, \underline{\mathbf{R}}, t) \right| \Phi_{\underline{\mathbf{R}}}(t) \right\rangle_{\underline{\mathbf{r}}} \quad (7)$$

is form-invariant under the gauge-transformation $\Phi_{\underline{\mathbf{R}}}(\underline{\mathbf{r}}, t) \rightarrow \tilde{\Phi}_{\underline{\mathbf{R}}}(\underline{\mathbf{r}}, t) = \exp(i\theta(\underline{\mathbf{R}}, t))\Phi_{\underline{\mathbf{R}}}(\underline{\mathbf{r}}, t)$, $\chi(\underline{\mathbf{R}}, t) \rightarrow \tilde{\chi}(\underline{\mathbf{R}}, t) = \exp(-i\theta(\underline{\mathbf{R}}, t))\chi(\underline{\mathbf{R}}, t)$, whereas $\epsilon_{gd}(\underline{\mathbf{R}}, t)$, defined as

$$\epsilon_{gd}(\underline{\mathbf{R}}, t) = \left\langle \Phi_{\underline{\mathbf{R}}}(t) \left| -i\partial_t \Phi_{\underline{\mathbf{R}}}(t) \right\rangle_{\underline{\mathbf{r}}} \quad (8)$$

is the part that depends on the choice of the gauge. Here, $\langle \dots \rangle_{\underline{\mathbf{r}}}$ denotes an inner product over the electronic variables only.

Why is this representation of the correlated electron-nuclear many-body problem exciting? The wave-function $\chi(\underline{\mathbf{R}}, t)$ that satisfies the exact nuclear equation of motion (4) leads to an N -body density $\Gamma(\underline{\mathbf{R}}, t) = |\chi(\underline{\mathbf{R}}, t)|^2$ and an N -body current density $\mathbf{J}_\nu(\underline{\mathbf{R}}, t) = \text{Im}(\chi^* \nabla_\nu \chi) + \Gamma(\underline{\mathbf{R}}, t) \mathbf{A}_\nu$ which reproduce the true nuclear N -body density and current density obtained from the full wave-function $\Psi(\underline{\mathbf{r}}, \underline{\mathbf{R}}, t)$ [5]. In this sense, $\chi(\underline{\mathbf{R}}, t)$, can be viewed as the proper nuclear wave-function. The time evolution of $\chi(\underline{\mathbf{R}}, t)$, on the other hand, is completely determined by the TDPEs, $\epsilon(\underline{\mathbf{R}}, t)$, and the vector potential, $\mathbf{A}_\nu(\underline{\mathbf{R}}, t)$. Moreover, these potentials are *unique* up to within a gauge transformation. This uniqueness is straightforwardly proven by following the steps of the current-density version [6] of the Runge-Gross theorem [7]. In other words, if one wants a TDSE (4) whose solution $\chi(\underline{\mathbf{R}}, t)$ yields the true nuclear N -body density and current density, then the potentials appearing in this TDSE are (up to within a gauge transformation) uniquely given by Eqs. (5-8); there is no other choice. This also implies, that the gradient of this exact TDPEs *is the only correct force on the nuclei* in the classical limit (plus terms arising from the vector potential, if those cannot be gauged away). The goal of this Letter is to find out how this exact TDPEs looks like when one has strong non-adiabatic couplings in the traditional expansion in BO states. One major result will be that the exact TDPEs shows a nearly discontinuous step whenever the nuclear wave-packet splits in the vicinity of an avoided crossing of the BOPES.

To study the exact TDPEs we first of all need a problem that is simple enough to allow for a numerically exact solution and that nevertheless exhibits the characteristic features associated with strong non-adiabatic couplings, such as the splitting of the nuclear wave packet.

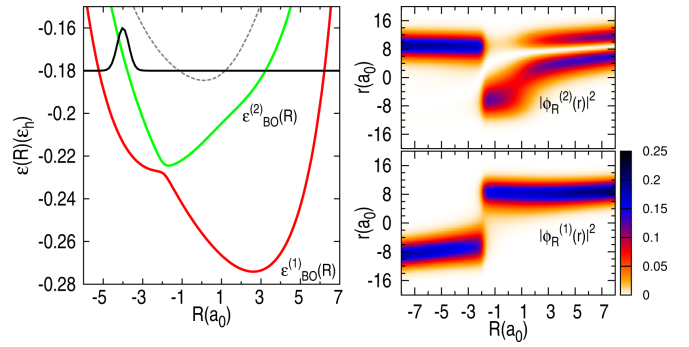


FIG. 1. Left: The first two BOPEs (indicated in the figure) together with the 3rd BOPEs (black dashed-line) and the initial nuclear wave-function (black solid-line). Right: Adiabatic electronic conditional densities as indicated in the figures

For this purpose we employ the model of Shin and Metiu [8]. It consists of three ions and a single electron. Two ions are fixed at a distance of $L = 19.0 a_0$, the third ion and the electron are free to move in one dimension along the line joining the two fixed ions. The Hamiltonian of this system reads

$$\hat{H}(r, R) = -\frac{1}{2} \frac{\partial^2}{\partial r^2} - \frac{1}{2M} \frac{\partial^2}{\partial R^2} + \frac{1}{|L/2 - R|} + \frac{1}{|L/2 + R|} - \frac{\text{erf}\left(\frac{|R-r|}{R_f}\right)}{|R-r|} - \frac{\text{erf}\left(\frac{|r-L/2|}{R_r}\right)}{|r-L/2|} - \frac{\text{erf}\left(\frac{|r+L/2|}{R_l}\right)}{|r+L/2|} \quad (9)$$

Here, the symbols $\underline{\mathbf{r}}$ and $\underline{\mathbf{R}}$ are replaced by r and R , the coordinates of the electron and the movable nucleus measured from the center of the two fixed ions. $M = 1836$ a.u. and we choose $R_f = 5.0 a_0$, $R_l = 3.1 a_0$ and $R_r = 4.0 a_0$ such that the first BOPEs, $\epsilon_{BO}^{(1)}$, is strongly coupled to the second BOPEs, $\epsilon_{BO}^{(2)}$, around the avoided crossing at $R_{ac} = -1.90 a_0$ and there is a weak coupling to the rest of the surfaces. The first three BOPEs are shown in Fig. 1 (left panel), together with the BO conditional electronic densities $|\phi_R^{(1)}(r)|^2$ and $|\phi_R^{(2)}(r)|^2$ (right panels). As expected, $|\phi_R^{(1)}(r)|^2$ and $|\phi_R^{(2)}(r)|^2$ exhibit abrupt changes, along the R -axis, at the position of the avoided crossing, R_{ac} : $|\phi_R^{(1)}(r)|^2$ switches from being localized around the fixed ion on the left ($r = -9.5 a_0$), to be localized around the one on the right ($r = 9.5 a_0$); $|\phi_R^{(2)}(r)|^2$ on the other hand, presents a single-peak structure for $R < R_{ac}$ and a double-peak structure for $R > R_{ac}$.

We suppose that the system is initially excited to $\epsilon_{BO}^{(2)}$ and the initial nuclear wave-function is a wave-packet with the width $\sigma = 1/\sqrt{2.85}$, centered at $R = -4.0 a_0$ (see Fig. 1, black solid-line), i.e., the initial full wave-function is $\Psi_0(r, R) = A e^{-(R-4)^2/\sigma^2} \phi_R^{(2)}(r)$ with A being a normalization constant. Starting with $\Psi_0(r, R)$ as initial state, we propagate the TDSE, nu-

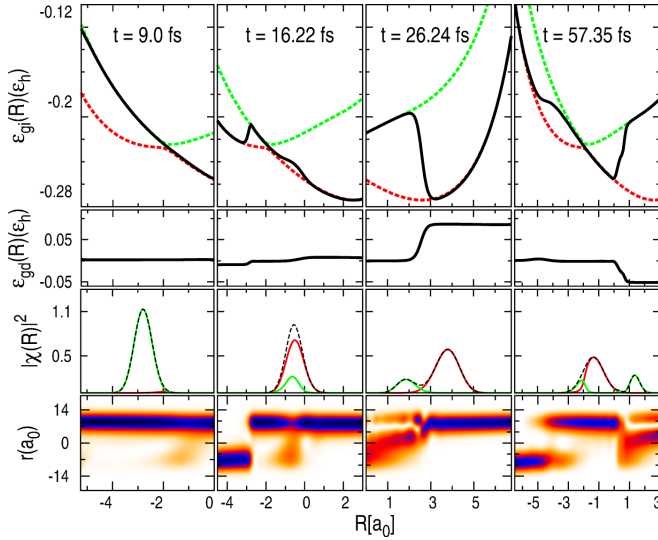


FIG. 2. First panel (top): The gauge independent part of the TD PES (black solid-line) plotted at four different times (indicated), $\epsilon_{BO}^{(1)}$ (red dashed-line) and $\epsilon_{BO}^{(2)}$ (green dashed-line). Second panel (from the top): the gauge dependent part of the TD PES is plotted at the same times. Third panel (from the top): the exact nuclear density (black dashed-line) is shown together with $|F_1(R, t)|^2$ (red solid-line) and $|F_2(R, t)|^2$ (green solid-line). Lowest panel: the exact time-dependent electronic conditional density, $|\Phi_R(r, t)|^2$, is plotted. The color range is the same as Fig. 1.

merically exactly, to obtain the full molecular wavefunction $\Psi(r, R, t)$ and from it we calculate, as discussed in Ref. [5], the TD PES in the gauge where the vector potential is zero. Hence, the TD PES is the only potential acting on the nuclear sub-system. In the upper panel of Fig. 2, the gauge-invariant part of the TD PES (7), ϵ_{gi} , is plotted (black solid-line) at four different times, along with the two lowest BO PESs, $\epsilon_{BO}^{(1)}$ (red dashed-line) and $\epsilon_{BO}^{(2)}$ (green dashed-line). In the second panel (from the top), the gauge-dependent part of the TD PES (8), ϵ_{gd} , is plotted at the same times. In the third panel (from the top), the exact nuclear density (black dashed-line), $|\chi(R, t)|^2$, is shown together with the absolute value squared of the projection of the full wavefunction on the first and second BO electronic states, i.e., $|F_1(R, t)|^2 = |\int dr \phi_R^{(1)*}(r) \Psi(r, R, t)|^2$ (red solid-line) and $|F_2(R, t)|^2 = |\int dr \phi_R^{(2)*}(r) \Psi(r, R, t)|^2$ (green solid-line). In the lowest panel, $|\Phi_R(r, t)|^2$ is presented.

At the initial time ($t = 0$), due to the choice of the initial state, the TD PES coincides with $\epsilon_{BO}^{(2)}$. Since $\Psi_0(r, R)$ is not an eigenstate of the Hamiltonian (9), it evolves in time. At $t = 9.0 fs$, ϵ_{gi} coincides with $\epsilon_{BO}^{(2)}$ for $R < R_{acr}$, goes smoothly through the avoided crossing region and follows $\epsilon_{BO}^{(1)}$ for $R > R_{acr}$, resembling the *diabatic* PES of state 2 in Ref. [8], in which the electron interacts with the fixed ion on the right ($r = 9.5 a_0$) and with the moving

ion, but not with the fixed ion on the left ($r = -9.5 a_0$). As ϵ_{gd} is constant in this region (Fig. 2), the TD PES is identical with ϵ_{gi} [9]. The nuclear wave-packet is driven by the TD PES to spread towards the avoided crossing of two BO PESs, where a significant non-adiabatic transition happens and the exact nuclear density splits. Already at this moment, a slight transition of the nuclear wave-packet to the lower surface is visible around the avoided crossing. At later times, e.g., $t = 16.22 fs$, $t = 26.24 fs$ and $t = 57.35 fs$, far from the avoided crossing, ϵ_{gi} contains steps that connect its different pieces that are on top of different BO PESs in different slices of R -space. In the region around R_{acr} , it follows the diabatic surface that passes smoothly through the avoided crossing. On the other hand, ϵ_{gd} is piecewise constant and presents similar steps as ϵ_{gi} . Therefore, the TD PES, $\epsilon_{gi} + \epsilon_{gd}$, preserves the features mentioned before, i.e., (i) far from the avoided crossing, it presents steps that connect the regions in R -space in which the TD PES has the shape of one BO PES to the regions in which it has the shape of the other BO PES; (ii) around the avoided crossing, it follows the diabatic surface that smoothly connects one BO PES to the other.

The exact TD PES represented in Fig. 2 can be viewed from a different perspective. The nuclear wave-packet from a semi-classical point of view can be represented as an ensemble of classical trajectories, along which point-particles evolve under the action of a classical force which is the gradient of ϵ_{gi} . According to our observations, on different sides of a step such a force is calculated from different BO PESs. This is reminiscent of the *jumping between the adiabatic surfaces* in algorithms such as Tully's surface hopping [10, 11]. However, while Tully surface hopping is a stochastic algorithm, the jumps in the exact TD PES correspond to an exact solution of the TDSE. When the time-dependent vector potential can not be set to zero, a gauge can be chosen in which ϵ_{gd} is zero and a time-dependent vector potential together with ϵ_{gi} specifies the classical force that the nuclei experience in different slices of R -space. Investigating ϵ_{gi} together with the time-dependent vector potential for a wide range of situations may help to improve the existing semi-classical procedures to simulate non-adiabatic nuclear dynamics.

The exact time-dependent electronic conditional density, shown in the lower panels of Fig. 2 at different times, behaves similarly to the TD PES: (i) it smoothly connects a $|\phi_R^{(2)}(r)|^2$ -like structure, by crossing R_{acr} , with a $|\phi_R^{(1)}(r)|^2$ -like structure, or vice versa, presenting a diabatic behavior, e.g. at $t = 9.0 fs$; (ii) it displays abrupt changes, between regions that piecewise match different adiabatic conditional densities.

In order to analyze the behavior of the TD PES, we rewrite it by expanding the exact electronic conditional wave-function in terms of the adiabatic electronic states

[5]. Due to the choice of the parameter in the Hamiltonian, we only need to include the first two BO states, then

$$\Phi_R(r, t) = C_1(R, t)\phi_R^{(1)}(r) + C_2(R, t)\phi_R^{(2)}(r). \quad (10)$$

We expand the full electron-nuclear wave-function in the same basis,

$$\Psi(r, R, t) = F_1(R, t)\phi_R^{(1)}(r) + F_2(R, t)\phi_R^{(2)}(r), \quad (11)$$

where the expansion coefficients, F_k 's and C_k 's, are related as

$$C_k(R, t) = \frac{F_k(R, t)}{\chi(R, t)} = \frac{e^{-i\theta(R, t)} F_k(R, t)}{\sqrt{|F_1(R, t)|^2 + |F_2(R, t)|^2}}. \quad (12)$$

Here, θ is the phase of the exact nuclear wave-function and we have used the relation $|\chi(R, t)|^2 = |F_1(R, t)|^2 + |F_2(R, t)|^2$, determined by $\int dr |\Psi(r, R)|^2$ using Eq. (11) and the orthonormality of the adiabatic states. By using Eqs. (5) and (10), we rewrite $\epsilon_{gi}(R, t)$ and $\epsilon_{gd}(R, t)$ in terms of $\epsilon_{BO}^{(k)}(R)$ and $C_k(R, t)$ ($k = 1, 2$)

$$\epsilon_{gi}(R, t) = \sum_{k=1,2} |C_k(R, t)|^2 \epsilon_{BO}^{(k)}(R) \quad (13)$$

$$\epsilon_{gd}(R, t) = \sum_{k=1,2} |C_k(R, t)|^2 \dot{\gamma}_k(R, t), \quad (14)$$

where γ_1 and γ_2 are the phases of C_1, C_2 . In Eq. (13), all terms of $\mathcal{O}(M^{-1})$ have been neglected and it only contains BOPEs which are the leading terms responsible for the shape of $\epsilon_{gi}(R, t)$, especially far from the avoided crossing where the NACs are small. The gauge-dependent term is written in terms of the time derivative of the phases, $\dot{\gamma}_1$ and $\dot{\gamma}_2$. $|C_1|^2$ and $|C_2|^2$ vary between 0 and 1 and $|C_1|^2 + |C_2|^2 = 1$ by virtue of the PNC. Therefore, as Eq. (13) suggests, in the region where $\epsilon_{gi}(R, t)$ coincides with $\epsilon_{BO}^{(1)}(R)$, the corresponding expansion coefficient $|C_1|^2$ is close to one while $|C_2|^2$ is close zero and vice versa. We have observed (Eq. (12)) that at R_0 , the cross-over of $|F_1|$ and $|F_2|$ where $|F_1(R_0, t)| = |F_2(R_0, t)| = |X(t)|$, $|C_1|^2$ and $|C_2|^2$ are always equal to 1/2 and R_0 is the center of the region where steps form. Moving away from this point, one of the $|C_k|^2$'s becomes dominant (Fig. 3) and $\epsilon_{gi}(R, t)$ lies on top of the corresponding BOPEs.

To elaborate on how the TDPEs switches between the two adiabatic states, we Taylor expand $|C_k(R, t)|^2$ around R_0 and keep only up to the linear order terms

$$\left| C_2(R, t) \right|^2 = [1 \pm \alpha(t)(R - R_0)]/2, \quad (15)$$

where

$$\alpha(t) = \frac{(\nabla_R |F_1(R, t)|)_{R_0} - (\nabla_R |F_2(R, t)|)_{R_0}}{|X(t)|}. \quad (16)$$

Eq. (15), using the relation $0 \leq |C_k|^2 \leq 1$ ($k = 1, 2$) or equivalently $|R - R_0| \leq \alpha^{-1}$, estimates the width of the region, ΔR , where the switching between BOPEs occurs with $\frac{2}{\alpha}$, i.e., $\Delta R = \frac{2}{\alpha}$. Hence, the larger the values of α , the sharper the steps become.

As an example, we discuss the TDPEs at $t = 31.87$ fs in Fig. 3. As it is seen, ϵ_{gi} switches from $\epsilon_{BO}^{(1)}(R)$ to $\epsilon_{BO}^{(2)}(R)$ over the region where $|F_1|$ and $|F_2|$ cross (see the bottom plot). As $|F_1|$ and $|F_2|$ have opposite slopes and cross where they are small, α is large yielding a small ΔR . Outside the switching region, one of the $|C_k|^2$'s becomes dominant. Interestingly, the exact electron-nuclear density contains signatures of the behavior ϵ_{gi} , i.e., where ϵ_{gi} coincides with $\epsilon_{BO}^{(1)}(R)$, presents one peak in analogy with $|\phi_R^{(1)}(r)|^2$ (see Fig. 1), while, where $\epsilon_{gi}(R, t)$ follows $\epsilon_{BO}^{(2)}(R)$, it displays two peaks, like $|\phi_R^{(2)}(r)|^2$ (Fig. 1) The step of ϵ_{gi} in the intermediate region is indicated by scars in the full electron-nuclear density.

In conclusion, we have presented generic features of the exact TDPEs for situations in which, according to the standard BO expansion framework, significant non-adiabatic transitions occur and the nuclear wave-packet splits at the avoided crossing of two BOPEs. For the 1D model system studied here, the TDPEs is the only potential that governs the dynamics of the nuclear wave-function (the vector potential can be gauged away) and provides us with an alternative way of visualizing and interpreting the non-adiabatic processes. We have shown that the gauge-invariant part of the TDPEs, $\epsilon_{gi}(R, t)$, is characterized by two generic features: (i) in the vicinity of the avoided crossing, $\epsilon_{gi}(R, t)$, be-

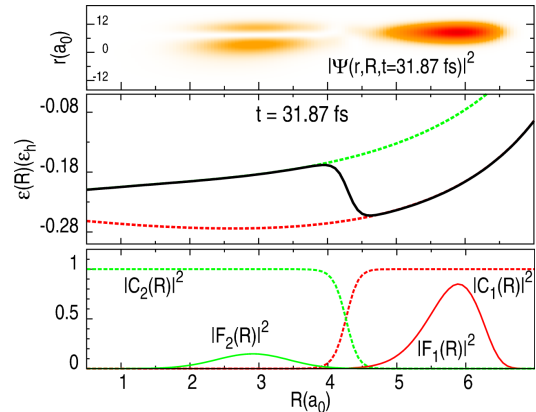


FIG. 3. Top: the full electron-nuclear density at the $t = 31.87$ fs. Middle: a snapshot of the gauge invariant part of the TDPEs (solid black line) at the $t = 31.87$ fs. For reference, $\epsilon_{BO}^{(1)}$ (red dashed-line) and $\epsilon_{BO}^{(2)}$ (green dashed-line) are shown. Bottom: Expansion coefficients (indicated in the figure) of the (two states) adiabatic expansion of the full wave-function and the exact electronic conditional wave-function (see the text) at the $t = 31.87$ fs.

comes identical with a diabatic PES in the direction of the wave-packet motion, (ii) far from the avoided crossing, $\epsilon_{gi}(R, t)$, as a function of R , is piecewise identical with different BOPEs and exhibits nearly discontinuous steps in between. The latter feature holds after the wave-packet branches and leaves the avoided crossing. The gauge-dependent part, $\epsilon_{gd}(R, t)$, on the other hand, is piecewise constant in the region where $\epsilon_{gi}(R, t)$ coincides with different BOPEs. Hence $\epsilon_{gd}(R, t)$ has little effect on the gradient of the total TDPEs, but may shift the BOPEs-pieces of $\epsilon_{gi}(R, t)$ by different constants causing the exact TDPEs to be piecewise parallel to the BOPEs. These features of the TDPEs support the use of diabatic surfaces as the driving potential when a wave-packet approaches a region of strong NAC. Moreover, they are in agreement with the semi-classical picture of non-adiabatic nuclear dynamics that suggests to calculate the classical forces acting on the nuclei according to *the gradient of only one of the BOPEs*. We expect that these findings will ultimately lead to improved algorithms for the mixed quantum-classical treatment of electrons and nuclei.

This study was supported by the European Commis-

sion within the FP7 CRONOS project (ID 280879).

-
- [1] W. Domcke and D. R. Yarkony, *Annu. Rev. Phys. Chem.* **63**, 325 (2012)
 - [2] M. Wohlgenuth and V. B.-K. and R. Mitrić, *J. Chem. Phys.* **135**, 054105 (2011) A. L. Sobolewski, W. Domcke, C. Dedonder-Lardeux, and C. Jouvet, *Phys. Chem. Chem. Phys.* **4**, 1093 (2002)
 - [3] T. S. Rose, M. J. Rosker, and A. H. Zewail, *J. Chem. Phys.* **91**, 7415 (1989) T. J. Martinez and R. D. Levine, *Chem. Phys. Lett.* **259**, 252 (1996) G. Hanna and R. Kapral, *J. Chem. Phys.* **122**, 244505 (2005)
 - [4] A. Abedi, N. T. Maitra, and E. K. U. Gross, *Phys. Rev. Lett.* **105**, 123002 (2010)
 - [5] A. Abedi, N. T. Maitra, and E. K. U. Gross, *J. Chem. Phys.* **137**, 22A530 (2012)
 - [6] S. K. Ghosh and A. K. Dhara, *Phys. Rev. A* **38**, 1149 (1988)
 - [7] E. Runge and E. K. U. Gross, *Phys. Rev. Lett.* **52**, 997 (1984)
 - [8] S. Shin and H. Metiu, *J. Chem. Phys.* **102**, 23 (1995)
 - [9] In Fig. 2, curves representing ϵ_{gd} have been rigidly shifted along the energy axis
 - [10] J. Tully and R. Preston, *J. Chem. Phys.* **55**, 562 (1971)
 - [11] R. K. S. Nielsen and G. Ciccotti, *J. Chem. Phys.* **112**, 6543 (2000)